Parametric pairs in antiferromagnet with easy plane anisotropy

V. I. Ozhogin and A. Yu. Yakubovskiĭ

I. V. Kurchatov Institute of Atomic Energy
(Submitted February 5, 1974)
Zh. Eksp. Teor. Fiz. **67**, 287–308 (July 1974)

The threshold amplitudes for parametric excitation (by parallel pumping) of wave pairs of normal modes of various nature are calculated for antiferromagnets with anisotropy of the easy plane type by taking exchange, Dzyaloshinskiĭ, hyperfine, and magnetoelastic interactions into account. An intermediate transformation in which the symmetry of the system is taken into account is employed when nuclear spin waves are introduced, and this simplifies the calculations considerably. Normal magnetoelastic oscillation modes, including the "intersection point," are found. In all cases the exchange and Dzyaloshinskiĭ interactions decrease the threshold amplitudes. The threshold microwave magnetic field values $h_c^{(1,2)}$ observed experimentally in $MnCO_3$ at $T=1.55$–$4.2\,°K$, $H_0=0$–1.5 kOe and $\nu_0 \approx 9.3$ GHz are interpreted at the result of excitation, $h_c^{(1)}$ being attributed to excitation of electron-nuclear spin pairs, and $h_c^{(2)}$ to excitation of "nondegenerate" normal magnetoelastic oscillation pairs. The nonlinear process observed at $\nu_0=875$ MHz and $h>0.06$ Oe is ascribed to excitation of nuclear-nuclear spin-wave pairs. It is suggested that an electron-nuclear three-particle relaxation mechanism exists.

1. INTRODUCTION

In antiferromagnets (AF) the interaction of the system of electron spins (E) with the system of nuclei (N) spins and with the elastic deformations (S) of the lattice leads to a mutual influence of the systems which is much stronger than in ferrites, owing to the participation of the exchange interaction, which as a rule is quite large. This mutual influence is subdivided into "static" and "dynamic" components. The first is calculated at "frozen-in" N and S subsystems and leads, in particular, to the appearance of additional terms in the expressions for the antiferromagnetic-resonance (AFMR) frequencies. The second causes a mixing of the linear vibrations of the subsystems, which is stronger the smaller the difference between the energies of the unperturbed oscillations.

From the experimental point of view, the study of these effects is most convenient in AF with easy-plane anisotropy (AFEP)[1], such as $MnCO_3$, $FeBO_3$, and others. In these substances, one of the branches of the electron spin wave spectrum is quasiferromagnetic (QF)[2b] and has energies of the same order as in ferrites at moderate magnetic fields. Therefore the exchange-enhanced influence of the hyperfine and magnetoelastic interactions on the QF branch is relatively large.

The first investigations of the static manifestation of the hyperfine and magnetoelastic interactions in AFEP were carried out in[3,4]. The dynamic manifestation of the hyperfine interaction leads to nuclear spin waves[5], and in particular to a shift of the NMR frequency[6]. The strong dependence of the speed of sound in AFEP on the magnetic field, which was observed in[7,8c], is the consequence of the dynamic magnetoelastic interaction of the electron spin waves with the phonons. The nuclear-like spin waves contain an appreciable admixture of electronic components, and therefore interact also with phonons, so that analogous effects are produced in the other frequency region[9].

The study of the most interesting of the nonlinear dynamic phenomena in AF, namely parallel pumping, was initiated by investigations of $RbMnF_3$[10a] and $CsMnF_3$[11,8a]1). The presence of hyperfine and magnetoelastic interactions greatly broadens the circle of the possible parametric processes, and the exchange enhancement can facilitate their experimental observation. In this paper we calculate the threshold amplitudes of the parallel-pump field for the main parametric processes in AFEP. The experimental study of the excitation of pairs of quasiparticles of different types was undertaken on $MnCO_3$, which is the typical AFEP (with Dzyaloshinskiĭ interaction), in which the hyperfine interaction is large[3] and the magnetoelastic interaction is noticeable[3,6,9].

2. THEORY

2A. Model and Calculation Scheme

We consider the simplest AFEP model that takes into account the effects of hyperfine and magnetoelastic interactions. It consists of the following:

a) An E-subsystem, namely two sublattices of electron spins with exchange, anisotropy, and Dzyaloshinskiĭ interactions (only between the nearest neighbors) and with interaction with the external field **H**.

b) An N subsystem, namely two nuclear-spin sublattices, each of which is coupled by hyperfine interaction only with the spin of "its own" electron (EN interaction).

c) An S subsystem, namely an elastic continuum of the lattice, which for simplicity is assumed to be cubic and elastically isotropic (i.e., the phonon velocity v_S depends only on the phonon polarization s and not on the direction of its wave vector **k**).

We shall take into account only the cubic-symmetry part of the single-ion magnetostriction[12-14] in the magnetoelastic (ES) interaction, but without the magnetoelastic isotropy ($B_1 \neq B_2$). With an eye at application to rhombohedral AFEP, the corresponding expression for the energy will be rewritten in a coordinate system in which the body diagonal of the cube is perpendicular to the easy plane: [111] ∥ z ∥ C_3 (see[13,15]).

The Hamiltonian of the system in this model is written in the form of a sum of the energies of the E, N, and S subsystems and the energies of their interaction (see the Appendix):

$$\mathcal{H}=\mathcal{H}_{EE}+\mathcal{H}_{NN}+\mathcal{H}_{SS}+\mathcal{H}_{EN}+\mathcal{H}_{ES}+\mathcal{H}_{NS}. \quad (1)$$

The most interesting case for AFEP is when the constant external field $\mathbf{H}_0$ lies in the easy plane. Directing the x axis along $\mathbf{H}_0$ and the z axis along the difficult axis of the crystal, we choose auxiliary systems with quantization axes along the equilibrium magnetizations. With the aid of the Holstein-Primakoff transformation and the Fourier transformation, we change over from the electron spin operators $\hat{S}_{j\nu}$ to the Bose operators $a^{\pm}_{\nu e\mathbf{k}}$, and analogously from the nuclear spin operators $\hat{I}_{j\nu}$ to $a^{\pm}_{\nu n\mathbf{k}}$ ($\nu = 1, 2$). We express $\mathscr{H}_{SS}$ and $\mathscr{H}_{ES}$ in terms of the phonon operators $b^{\pm}_{s\mathbf{k}}$. This enables us to rewrite (1) in the form

$$\mathscr{H}=\mathscr{H}_0+\mathscr{H}_1+\mathscr{H}_2+\mathscr{H}_3+\mathscr{H}_4+\mathscr{H}', \tag{2}$$

where the index of each term denotes each order in the Bose operators $a^{\pm}_{\nu e\mathbf{k}}$, $a^{\pm}_{\nu n\mathbf{k}}$, and $b^{\pm}_{s\mathbf{k}}$, while $\mathscr{H}'$ describes a perturbation that depends explicitly on the time.

From the condition $\mathscr{H}_1 = 0$ we obtain the equilibrium state, and then we separate the part quadratic in the Bose operators; this part is in turn conveniently represented in the form

$$\mathscr{H}_2=\mathscr{H}^{(2)}_{ee}+\mathscr{H}^{(2)}_{en}+\mathscr{H}^{(2)}_{pp}+\mathscr{H}^{(2)}_{ep}+\mathscr{H}^{(2)}_{nn}, \tag{3}$$

where the subscript e (electron), n (nuclear), and p (phonon) correspond to the operators $a^{\pm}_{\nu e\mathbf{k}}$, $a^{\pm}_{\nu n\mathbf{k}}$, and $b^{\pm}_{s\mathbf{k}}$. We diagonalize the term $\mathscr{H}^{(2)}_{ec}$

$$\mathscr{H}^{(2)}_{ee}=\hbar\sum_{\nu\mathbf{k}}\omega_{\nu\mathbf{k}}c^{+}_{\nu e\mathbf{k}}c_{\nu e\mathbf{k}} \tag{4}$$

with the aid of the transformation (the matrix $\mathbf{S}$ is written out in (A.10))

$$\mathrm{X}_{ae}=\mathrm{S}\mathrm{X}_{ce}, \tag{5a}$$

$$\mathrm{X}_{ae}\equiv(a_{1e\mathbf{k}}, a_{2e\mathbf{k}}, a^{+}_{1e-\mathbf{k}}, a^{+}_{2e-\mathbf{k}})^{T}, \tag{5b}$$

$$\mathrm{X}_{ce}\equiv(c_{1e\mathbf{k}}, c_{2e\mathbf{k}}, c^{+}_{1e-\mathbf{k}}, c^{+}_{2e-\mathbf{k}})^{T}. \tag{5c}$$

In the subsequent transformations it is useful to take into account the following physical circumstance. If we write out the Landau-Lifshitz equations for the two electron-spin sublattices, then it turns out that the quantities (μ_{ey}, μ_{ez}, λ_{ex}) oscillate with frequencies $\omega_{1\mathbf{k}}$ (QF mode) and the quantities (μ_{ex}, λ_{ey}, λ_{ez}) oscillate with frequencies $\omega_{2\mathbf{k}}$ (quasiantiferromagnetic (QAF) mode). Here $\boldsymbol{\mu}_e$ and $\boldsymbol{\lambda}_e$ are time-dependent small parts of the variables $\mathbf{M}_e \equiv \mathbf{M}_{e1} + \mathbf{M}_{e2}$ and $\mathbf{L}_e = \mathbf{M}_{e1} - \mathbf{M}_{e2}$, where $\mathbf{M}_{e\nu}$ is the magnetization of the ν-sublattice of the electron spins ($\nu = 1, 2$).

Introducing analogous variables $\mathbf{M}_n$ and $\mathbf{L}_n$ for the nuclear sublattices and writing down the general expressions of motion[5], we note that the system of 12 equations breaks up into two subsystems of six equations each. The first describes the oscillations of the "QF variables" (μ_{ey}, μ_{ez}, λ_{ex}, μ_{ny}, μ_{nz}, λ_{nx}), which are coupled by the hyperfine interaction, and leads to two QF branches of the spin-wave spectrum—quasielectron (e) and quasinuclear (n). The second group of six equations describes the QAF branches (e and n) of the spin waves (see also[16]).

When we consider the oscillations of the electron subsystem without allowance for its coupling with the nuclear system, the separation of the variables (μ_{ey}, μ_{ez}, λ_{ex}) from the aggregate ($\boldsymbol{\mu}_{e1}$, $\boldsymbol{\mu}_{e2}$) is fully equivalent to the separation of the variables $c^{\pm}_{1e\mathbf{k}}$ from the aggregate ($a^{\pm}_{1e\mathbf{k}}$, $a^{\pm}_{2e\mathbf{k}}$), which is effected by means of the transformation (5). Therefore, when considering coupled oscillations in terms of creation and annihilation operators, it is convenient to introduce new (auxiliary) nuclear spin operators $c^{\pm}_{\nu n\mathbf{k}}$ with the aid of exactly the same transformation (5) which was used to introduce the operators $c^{\pm}_{\nu e\mathbf{k}}$:

$$\mathrm{X}_{an}=\mathrm{S}\mathrm{X}_{cn}, \tag{6}$$

where $\mathbf{X}_{an}$ and $\mathbf{X}_{cn}$ are formed in analogy with (5b) and (5c), and $\mathbf{S}$ is the same as in (5a).

As a result of this, and also of the transformation of $\mathscr{H}_{ES}$ to the variables $c^{\pm}_{\nu e\mathbf{k}}$ and $b^{\pm}_{s\mathbf{k}}$, we obtain an expression that is subject to final diagonalization:

$$\begin{aligned}\mathscr{H}_2=\hbar\sum_{\mathbf{k}}\sum_{\nu=1}^{2}\Big\{&\omega_{\nu\mathbf{k}}c^{+}_{\nu e\mathbf{k}}c_{\nu e\mathbf{k}}+E_{\nu\mathbf{k}}c^{+}_{\nu n\mathbf{k}}c_{\nu n\mathbf{k}}\\&+(F_{\nu\mathbf{k}}c_{\nu n\mathbf{k}}c_{\nu n\,-\mathbf{k}}+G_{\nu\mathbf{k}}c_{\nu e\mathbf{k}}c^{+}_{\nu n\mathbf{k}}+H_{\nu\mathbf{k}}c_{\nu e\mathbf{k}}c_{\nu n\,-\mathbf{k}}+\mathrm{H.c.})\\&+\sum_{s=1}^{3}[\omega_{s\mathbf{k}}b_{s\mathbf{k}}{}^{+}b_{s\mathbf{k}}+(D_{\nu s\mathbf{k}}c_{\nu e\mathbf{k}}-D^{*}_{\nu s\mathbf{k}}c^{+}_{\nu e-\mathbf{k}})(b_{s-\mathbf{k}}-b_{s\mathbf{k}}{}^{+})]\Big\}.\end{aligned} \tag{7}$$

This equation is convenient because the only directly coupled operators are $c^{\pm}_{\nu e\mathbf{k}}$ and $c^{\pm}_{\nu n\mathbf{k}}$ with identical ν, i.e., spin variables of like symmetry. The variables with unlike symmetry are coupled only via the phonons. The transformation (6) can greatly simplify a great variety of calculations for the oscillations in the EN system (for example, of the relaxation frequencies).

For the frequencies of the uncoupled oscillations we have at small $k \ll a^{-1}$ (a is of the order of the lattice constant):

$$\omega_{1\mathbf{k}}{}^2\equiv\omega_{m\mathbf{k}}{}^2=\gamma^2[H_0(H_0+H_D)+2H_E(H_N+H^{(1)}_{mes})+v_m{}^2k^2] \tag{8a}$$

for the QF mode and

$$\omega_{2\mathbf{k}}{}^2=\gamma^2[2H_EH_A+H_D(H_0+H_D)+2H_E(H_N+H^{(2)}_{mes})+v_m{}^2k^2] \tag{8b}$$

for the QAF mode;

$$v^2{}_m=v^2{}_{m\perp}\sin^2\theta_{\mathbf{k}}+v^2{}_{m\parallel}\cos^2\theta_{\mathbf{k}}, \tag{8c}$$

$$\omega_{s\mathbf{k}}=v_sk,\qquad v_1\equiv v_l,\qquad v_2=v_3\equiv v_t, \tag{8d}$$

$$\omega_{\nu n\mathbf{k}}=(E^2{}_{\nu\mathbf{k}}-F^2{}_{\nu\mathbf{k}})^{1/2}=\omega_n. \tag{8e}$$

Here $\theta_{\mathbf{k}}$ is the polar angle of $\mathbf{k}$, v_l and v_t are the longitudinal and transverse sound velocities, v_m is the "maximum velocity" of the magnons, and ω_n is the frequency of the unshifted NMR.

In our approximation (cubic approximation for the elastic subsystem) we have $H^{(1)}_{mes} = H^{(2)}_{mes}$ (cf.[4]; H_{mes} is the effective field of the static magnetoelastic interaction).

When EE interactions between only nearest neighbors are taken into account, the "maximum velocities" $v_{m\perp}$ and $v_{m\parallel}$ for the electron spin waves are uniquely determined[17b] by the effective exchange field (which can be calculated from the value of the static susceptibility χ).

2B. Spectrum of Normal Oscillations

The spectrum of the normal oscillations of the ENS system for the cubic AF was calculated by Fedders[14], and in some particular cases also by others[5,9,18]. We shall diagonalize the Hamiltonian (7) only for the case $\omega_{20} \gg \omega_{10}$, for in this case U_1, $V_1 \gg U_2$, V_2 (see (A.10)), so that we can neglect the coupling of the variables with different ν via the phonons. Assuming for simplicity $D_{2\mathbf{k}s} = 0$, we can in general neglect the QAF modes. The dispersion relation for the coupled ENS waves takes the form

$$[(\Omega^2-\Omega_{1e\mathbf{k}}^2)(\Omega^2-\omega_{s\mathbf{k}}^2)-K_{ES}\omega_{s\mathbf{k}}^2\omega_{1\mathbf{k}}^2](\Omega^2-\Omega_{1n\mathbf{k}}^2)+\omega_{1\mathbf{k}}^2\omega_n^2\omega_{sk}^2K_{EN}K_{ES}\approx 0, \tag{9}$$

where $\Omega_{1e\mathbf{k}}$ and $\Omega_{1n\mathbf{k}}^2$ are the roots of the dispersion equation for the coupled EN waves without allowance for the magnetoelastic interaction:

$$(\Omega^2-\omega^2_{1\mathbf{k}})(\Omega^2-\omega_n^2)\approx\omega^2_{1\mathbf{k}}\omega_n^2K_{EN}. \tag{10}$$

Here and in (9) the dynamic-coupling coefficients take the form

$$K_{ES}=\omega_E\omega_{med}/\omega^2_{1\mathbf{k}},\quad K_{EN}=\omega_E\omega_N/\omega^2_{1\mathbf{k}} \tag{9a}$$

(ω_{med} is the effective frequency of the dynamic magnetoelastic interaction).

From (10) follow the known relations [5]

$$\Omega_{1e\mathbf{k}}^2\approx\omega_{1\mathbf{k}}^2+\omega_N\omega_E\omega_n^2/\omega_{1\mathbf{k}}^2\approx\omega_{1\mathbf{k}}^2, \tag{11a}$$

$$\Omega_{1n\mathbf{k}}^2\approx\omega_n^2(1-\omega_E\omega_N/\omega_{1\mathbf{k}}^2). \tag{11b}$$

In the derivation of (9)—(11) we used the inequalities

$$\omega_E\gg\omega_{2\mathbf{k}}\gg\omega_{1\mathbf{k}}\gg\omega_n\gg\omega_N,\ \omega_{med}, \tag{12}$$

which are satisfied, for example, for $MnCO_3$ at helium temperatures in moderate fields H_0.

Figure 1 shows the part of the spectrum of the normal AFEP oscillations pertaining to the QF modes, constructed from formulas (8) and (11) (the numerical values correspond to the case of $MnCO_3$).

It follows from (9) and (10) that the coupling of the nuclear spin waves with the phonons (via the electron spins) is the strongest, as usual, at the "intersection point" $k = k_c^{(np)}$. On the other hand if $k \to 0$, then we obtain for the velocity of the quasisound waves

$$V_s=v_s[1-\omega_E\omega_{med}/(\omega_{10}^2-\omega_E\omega_N)]^{1/2}, \tag{13}$$

i.e., an expression that leads to an exchange-enhanced dependence of the speed of sound in AFEP on the magnetic field [7,8a]. From (13) and (8a) we obtain the curious fact that the presence of the N system does not influence the form of this dependence even at the lowest temperatures T, even though $k_c^{(np)}$ shifts with T.

Each of the three branches of the spectrum ($\Omega_{1\mathbf{k}}$, $\Omega_{2\mathbf{k}}$, $\Omega_{3\mathbf{k}}$) contains some admixture of electron-spin components, and consequently is coupled with the external field (including the alternating field). Therefore by parallel pumping at frequency ω_p it is possible in principle to excite any of the possible six pairs of elementary excitations with oppositely directed quasimomenta, if the energy conservation law is satisfied

$$\omega_p=\Omega_{\sigma\mathbf{k}}+\Omega_{\rho-\mathbf{k}}\quad(\sigma,\ \rho=1,\ 2,\ 3). \tag{14}$$

To determine the threshold amplitudes of these processes it is necessary to construct the normal oscillations of the system, described by the Hamiltonian (7). This problem is in the general case very cumbersome (especially at $k \sim k_c^{(np)}$), but for definite pump-frequency intervals it is possible to carry out a separate diagonalization of the hyperfine and magnetoelastic interactions in the AFEP.

2C. Parallel Pumping of ee, nn, and en Pairs of Spin Waves

We shall omit from (7) the terms containing the phonon operators $b_{s\mathbf{k}}^{\pm}$. The diagonalization of the remaining part is carried out by introducing the normal coordinates $\alpha_{\nu e\mathbf{k}}^{\pm}$ and $\alpha_{\nu n\mathbf{k}}^{\pm}$ with the aid of the transformation (A.14). In the concrete calculation of its coefficients, it is necessary to distinguish between three cases: I—low electron frequencies, $\omega_{\nu\mathbf{k}} \ll \omega_E/4$, and II—the simpler but less interesting case $\omega_{\nu\mathbf{k}} \lesssim \omega_E/4$ (see the Appendix). For $MnCO_3$ and $CsMnF_3$ we have $\omega_E/\gamma \sim 7\times 10^5$ Oe and $\omega_{20}/\gamma \sim 10^5$ Oe, so that in fields $H_0 \le 15$ kOe there is realized case I for $\nu = 1$ and case II for $\nu = 2$ [see (8)]. In case I, the formulas are relatively simple at not too small values of $\Omega_{\nu n\mathbf{k}} \gg \rho_\nu\omega_n$, and this condition, as a rule, is satisfied ($\rho_\nu \equiv (\omega_n\omega_N)^{1/2}/\omega_{\nu\mathbf{k}}$). For cubic AF (at $H_0 > H_{SF}$ they are similar to AFEP), in which the frequency ω_{20} is low as a rule (e.g., $RbMnF_3$), case I is realized for both ν.

In the calculation of the threshold amplitudes under parallel pumping, when $\mathbf{H} = (H_0 + h\cos\omega_p t,\ 0,\ 0)$, it suffices to retain in (2) only the perturbing terms $\mathscr{H}_3 + \mathscr{H}'$. Allowance for $\mathscr{H}_4$ is essential in the calculation of the state beyond threshold. Changing over in (7) and in $\mathscr{H}_3 + \mathscr{H}'$ to the normal-oscillation operators (for our purposes they can be regarded as c-numbers) and retaining only the terms that have a bearing on our problem, we obtain (σ, ρ = e, n)

$$\begin{aligned}\hbar^{-1}\mathscr{H}_{en}=&\Omega_{2e0}\alpha_{2e0}^{+}\alpha_{2e0}+\gamma h\cos(\omega_p t)R_0(\alpha_{2e0}^{+}+\alpha_{2e0})+\sum_{\rho,\mathbf{k}}\Omega_{1\rho\mathbf{k}}\alpha_{1\rho\mathbf{k}}^{+}\alpha_{1\rho\mathbf{k}}\\&+\Big\{\sum_{\sigma,\rho,\mathbf{k}}[\gamma h\cos(\omega_p t)F_{\mathbf{k}}^{(\sigma\rho)}-(\Phi_{\mathbf{k}}^{(\sigma\rho)}\alpha_{2e0}^{+}+\Psi_{\mathbf{k}}^{(\sigma\rho)}\alpha_{2e0})]\alpha_{1\sigma\mathbf{k}}^{+}\alpha_{1\rho-\mathbf{k}}^{+}+\mathrm{H.c.}\Big\}.\end{aligned} \tag{15}$$

Setting up the equations of motion and introducing in them the dissipation phenomenologically (see [10b,c]), we obtain for the threshold amplitudes h_c the expression

$$h_c^{(\sigma\rho)}=\frac{1}{\gamma}(\tilde{\eta}_{1\sigma\mathbf{k}}\tilde{\eta}_{1\rho\mathbf{k}})^{1/2}\left|F_{\mathbf{k}}^{(\sigma\rho)}+\frac{R_0\Phi_{\mathbf{k}}^{(\sigma\rho)}}{\Omega_{2e0}+\omega_p+i\tilde{\eta}_{2e0}}+\frac{R_0\Psi_{\mathbf{k}}^{(\sigma\rho)}}{\Omega_{2e0}-\omega_p-i\tilde{\eta}_{2e0}}\right|^{-1}. \tag{16}$$

Here $\mathbf{k}$ is determined by the equation $\omega_p = \Omega_{1\sigma\mathbf{k}} + \Omega_{1\rho-\mathbf{k}}$ and $\tilde{\eta}_{\nu\rho\mathbf{k}}$ are the relaxation frequencies (in [17b] they are designated $\eta_{\nu\rho\mathbf{k}}$) of the corresponding normal oscillations. In first-order approximation, the $\tilde{\eta}_{\nu\rho\mathbf{k}}$ can be expressed in terms of the relaxation frequencies $\eta_{\nu e\mathbf{k}} \equiv \eta_{\nu\mathbf{k}}$ and $\eta_{\nu n\mathbf{k}} \equiv \eta_n$ of the (dynamically) non-interacting oscillations of the electron and nuclear spins by differentiating (10) with a constant right-hand side.

At an arbitrary pump frequency, we confine ourselves to the product of the expression for the threshold of the excitation of only ee pairs ($\Omega_{2e0} \approx \omega_{20}$, $\tilde{\eta}_{2e0} \approx \eta_{20}$, $\tilde{\eta}_{1e\mathbf{k}} \approx \eta_{1\mathbf{k}}$):

$$\begin{aligned}\gamma h_c^{(ee)}=&2\eta_{1\mathbf{k}}\omega_p[(\omega_{20}^2-\omega_p^2+\eta_{20}^2)^2+4\omega_p^2\eta_{20}^2]^{1/2}\{[\gamma H_0(2\omega_{20}^2+\eta_{20}^2)\\&+\gamma H_D(\omega_{20}^2-\omega_p^2+\eta_{20}^2)]^2+\gamma^2(H_0+2H_D)^2\omega_p^2\eta_{20}^2\}^{-1/2}.\end{aligned} \tag{17}$$

At $\eta_{20} \ll \omega_{20}$ it practically coincides with that derived from the Landau-Lifshitz equation [2b].

The simplest expressions are obtained in the frequently encountered experimental situation $\omega_p \ll \Omega_{2e0} \approx \omega_{20}$ [17b] 2).

$$\gamma h_c^{(ee)}=\frac{2\omega_{1\mathbf{k}}^2}{\gamma(H_D+2H_0)Q_{1e\mathbf{k}}}, \tag{18a}$$

$$\gamma h_c^{(en)}=\frac{2\omega_{1\mathbf{k}}^2(\omega_{1\mathbf{k}}^2/\omega_N\omega_E-1)^{1/2}}{\gamma(H_D+2H_0)(Q_{1e\mathbf{k}}Q_{1n\mathbf{k}})^{1/2}}, \tag{18b}$$

$$\gamma h_c^{(nn)}=\frac{2\omega_{1\mathbf{k}}^2(\omega_{1\mathbf{k}}^2/\omega_N\omega_E-1)}{\gamma(H_D+2H_0)Q_{1n\mathbf{k}}}. \tag{18c}$$

Here $Q_{\nu\rho\mathbf{k}} \equiv \Omega_{\nu\rho\mathbf{k}}/2\tilde{\eta}_{\nu\rho\mathbf{k}}$ are the quality factors of the corresponding normal modes (they can be expressed in terms of $q_{1ek} \equiv \omega_{1k}/2\eta_{1k}$ and $q_n \equiv \omega_n/2\eta_n$, i.e., the Q's of the noninteracting vibrations). At $H_D = 0$, expressions (18) differ from those given in[10c] only in the notation. If identical $\mathbf{k}$ are ensured for all three cases by suitable choice of ω_p, then at $\omega_p \ll \omega_{20}$ there follows from (18) the curious relation

$$h_c^{(en)} = (h_c^{(ee)} h_c^{(nn)})^{1/2}. \tag{19}$$

In the derivation of (18) we neglected the dynamic magnetoelastic interaction. Therefore agreement between these formulas and experiment can be expected only if the values of $\mathbf{k}$ determined by the frequency condition are far enough from the points of intersection of the quasielectronic (Ω_{1ek}) and quasinuclear (Ω_{1nk}) branches with the phonon branches of the spectrum (i.e., from $\mathbf{k}_c^{(ep)}$ and $\mathbf{k}_c^{(np)}$, see Fig. 1).

2D. Parallel Pumping of Magnetoelastic Waves

We omit from (7) the terms containing the nuclear spin operators $c_{\nu nk}^{\pm}$. Being interested in AFEP and in $\mathbf{k}$ such that $\omega_{20} \gg \omega_{1k} \equiv \omega_{mk}$, we neglect in the remaining part the connection between the phonons and the QAF branch, i.e., we put $D_{2sk} = 0$. The diagonalization of the Hamiltonian

$$\hbar \sum_{\mathbf{k}} \left[\omega_{m\mathbf{k}} c_{m\mathbf{k}}^{+} c_{m\mathbf{k}} + \sum_{s=1}^{3} \omega_{s\mathbf{k}} b_{s\mathbf{k}}^{+} b_{s\mathbf{k}} + \sum_{s=1}^{3} (D_{1s\mathbf{k}} c_{1\mathbf{k}} - D_{1s\mathbf{k}}^{*} c_{1-\mathbf{k}}^{+})(b_{s-\mathbf{k}} - b_{s\mathbf{k}}^{+}) \right] \tag{20}$$

is carried out with the aid of the transformation (A.16).

The natural frequencies of the coupled magnetoelastic oscillations are determined by the solutions of the dispersion equation

$$(\Omega^2 - \omega_{m\mathbf{k}}^2)(\Omega^2 - \omega_{s\mathbf{k}}^2) = \omega_E \omega_{med} v_s^2 \mathbf{k}^2, \tag{21}$$

where $4|D_{1sk}|^2 \omega_{mk} \equiv \omega_E \omega_{med}^{1s} v_s k$ defines the effective frequency $\omega_{med}^{1s} \equiv \omega_{med}$ of the dynamic magnetoelastic coupling, which depends on the direction of the unit vector $\mathbf{k}/k$ and on the polarization s of the phonon interacting with the QF electronic spin wave.

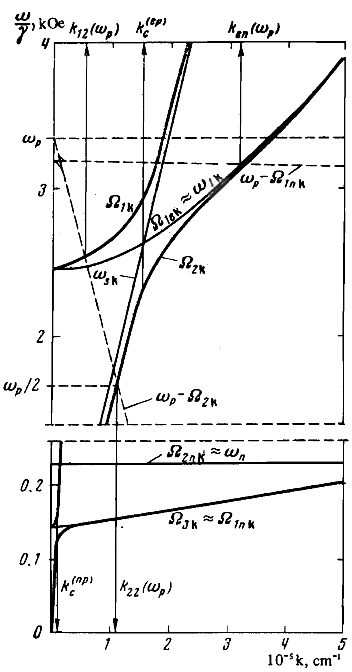

FIG. 1. Spectrum of $MnCO_3$ at $H_0 = 0.5$ kOe, $T = 1.7°K$, $H_D = 4.4$ kOe, $\omega_E\omega_N/\gamma^2 = 5.8\ T^{-1}$ kOe, $\omega_E\omega_{mes}/\gamma^2 = 0.3\ kOe^2$, $\omega_E\omega_{med}/\gamma^2 = 0.4\ kOe^2$, $v_m = 1.07 \times 10^5$ cm/sec, $v_s = 3.0 \times 10^5$ cm/sec. Pump frequency $\omega_p/\gamma = 3.3$ kOe.

The Hamiltonian of the problem, with allowance for the three-particle interaction responsible for the parallel pumping, acquires when expressed in terms with the operators of the normal magnetoelastic oscillations $\alpha_{\sigma k}^{\pm}$ the already known form (15) with the substitutions $1\sigma \to \sigma$ and $1\rho \to \rho$, and with the coefficients of (A.17); $\sigma, \rho = 1, 2$. At $\omega_p \ll \omega_{20}$, using (16), (21) and (A.16), and changing over from the Q's $Q_{\sigma k} \equiv \Omega_{\sigma k}/2\eta_{\sigma k}$ of the normal modes to the Q's $q_{mk} \equiv \omega_{mk}/2\eta_{mk}$ and $q_{sk} \equiv \omega_{sk}/2\eta_{sk}$ of the noninteracting magnons (m) and phonons (s), we obtain (in a form somewhat different than in[17c])

$$\gamma h_c^{(\sigma\sigma)} = \frac{2\omega_{1\mathbf{k}}^2}{q_{m\mathbf{k}}\gamma(H_D+2H_0)} \left[1 + \frac{q_{m\mathbf{k}}}{q_{s\mathbf{k}}} \frac{(\Omega_{\sigma\mathbf{k}}^2 - \omega_{1\mathbf{k}}^2)}{\omega_{m\mathbf{k}}^2 \omega_E \omega_{med}} \right], \quad \omega_p = 2\Omega_{\sigma\mathbf{k}}; \tag{22a}$$

$$\gamma h_c^{(12)} = \frac{2\omega_{1\mathbf{k}}^2}{q_{m\mathbf{k}}\gamma(H_D+2H_0)} \left\{ \left[1 + \frac{q_{m\mathbf{k}}}{q_{s\mathbf{k}}} \frac{(\Omega_{1\mathbf{k}}^2 - \omega_{1\mathbf{k}}^2)}{\omega_{m\mathbf{k}}^2 \omega_E \omega_{med}} \right] \times \left[1 + \frac{q_{m\mathbf{k}}}{q_{s\mathbf{k}}} \frac{(\omega_{m\mathbf{k}}^2 - \Omega_{2\mathbf{k}}^2)^2}{\omega_{m\mathbf{k}}^2 \omega_E \omega_{med}} \right] \right\}^{1/2}, \quad \omega_p = \Omega_{1\mathbf{k}} + \Omega_{2\mathbf{k}}. \tag{22b}$$

As in the preceding section, if ω_p is suitably chosen we obtain the relation

$$h_c^{(12)} = (h_c^{(11)} h_c^{(22)})^{1/2}.$$

In the case of maximum dynamic coupling of the magnons of the QF branch with the phonons, which occurs at $\omega_{mk} = \omega_{sk} \equiv \omega_c$, all three thresholds practically coincide at $(\omega_E\omega_{med})^{1/2} \ll 2\omega_c$:

$$h_c^{(11)} \approx h_c^{(22)} \approx h_c^{(12)} \approx \frac{\omega_p(2\eta_{1\mathbf{k}_c} + 2\eta_{s\mathbf{k}_c})}{\gamma(H_D+2H_{0c})} \equiv h_{cc}.$$

Here H_{0c} are the values of the external field at which $\omega_{mk} = \omega_{sk}$. We note that the expression for h_{cc} does not contain explicitly ω_{med} and can be obtained from the formula for the threshold of the excitation of the ee pairs[2b] by making the substitution $\Delta\omega_{1k_c} \equiv 2\eta_{1k_c} \to 2\eta_{1k_c} + 2\eta_{sk_c}$ (cf. (4.86) of[13]).

For AFEP, the general picture of the excitation of parametric pairs with allowance for the magnetoelastic interactions, is similar to that described by Comstock for ferrites[19]. However, the exchange amplification (the presence of ω_E in (9) and (22)) and the participation of the Dzyaloshinskiĭ interaction (which is sometimes large, for example $H_D = 100$ kOe in $FeBO_3$), make the AFEP experimentally convenient objects for the investigation of still unsolved general problems of parametric excitation of pairs of magnetoelastic oscillations.

Let us make a few remarks. Manganese carbonate is in closer agreement with the model in question than many other AFEP. A rigorous allowance for the elastic and magnetoelastic interactions (including the contribution of the distortion tensor) for rhombohedral $MnCO_3$ makes only the expression for $D_{\nu sk}$ somewhat more accurate, but hardly changes the expressions for $h_c^{(\alpha\rho)}$ at a scant angle $\psi \ll 1$ (by virtue of the structure of the coefficients $u_\pm$, $v_\pm$, $p_\pm$, $q_\pm$, see the Appendix). The real difficulties are more serious. The hard (with hysteresis) character of the excitation of, say, the ee pairs, observed in[17a, 20] (and for the case of ferrites in[21,22]) can call, even for the calculation of the thresholds (and not only the beyond-threshold state), for the allowance of four-particle interactions (for example, within the framework of the ideas developed in[23]. In addition, the small (in contrast to the ferrites) contribution of the dipole-dipole interaction to the formation of the spectrum of the spin waves in AFEP[2a] and the paired four-particle interaction can cause not one standing plane wave to be excited at $h = h_c$, but almost simultaneously a two-dimensional continuum in **k**-space (surface of ellipsoid of revolution for $MnCO_3$, see (8a)). This can greatly influence the interpretation of the experimental data (on the position of the phonon peaks on the $h_c(H_0)$ curves, etc.).

All the foregoing allows us to regard the cubic treatment[3)] of the magnetoelastic interaction (especially for the "rhombohedral" setting of the cube) as a sufficiently good approximation for a semiquantitative description of the thresholds of the parametric processes in $MnCO_3$.

3. EXPERIMENT

3A. Experimental Procedure

We investigated single-crystal samples in the form of plates, the largest of which measured $4 \times 3 \times 1$ mm (the AFMR line width was ≈ 100 Oe). The sample was glued to the bottom of a rectangular TE_{101}-mode reflex resonator with loaded $Q \simeq 1500$ and natural frequency $\nu_0 = \omega_0/2\pi = 9.3$ GHz. The threshold absorption was revealed on the oscilloscope screen by means of the distortion of the shape of the rectangular pulse reflected from the resonator. The absolute accuracy of the measurement of the amplitude of the threshold field h_c was $\pm 10\%$, and the relative accuracy was $\pm 2\%$.

Figure 2 shows a block diagram of a spectrometer for the study of parallel pumping in the 3-cm band. The power of the cw klystron was modulated by a p-i-n diode in such a way that microwave pulses of power ~ 10 mW and duration 10–1000 μsec, were applied to the input of a traveling wave tube (TWT) at a repetition frequency 5–50 Hz. These pulses were amplified in the TWT approximately 1000 times and were fed to the resonator. The signal reflected from the resonator was detected and observed on an oscilloscope screen.

The nonlinear processes in the 1 GHz frequency range, where parallel pumping of the nn pairs was expected, was investigated with the aid of the helicoidal resonator ($\nu_0 = 875$ MHz) mentioned in[10d].

A stationary magnetic field $\mathbf{H}_0 \parallel \mathbf{h} \perp C_3$ was produced by an electromagnet and was calibrated against AFMR in $MnCO_3$[3]. The accuracy with which H_0 was measured was 1%. The helium-bath temperature was varied between 1.55 and 4.2°K and was determined from the helium vapor pressure with an error ± 0.01°K.

3B. Measurement Results

When the pulse amplitude was increased to a certain value corresponding to the threshold intensity of the microwave magnetic field $h_c^{(1)}$, the pulse waveform became distorted (Figs. 3a and 3b) as a result of excitation of a certain parametric process in the sample. Further increase in the amplitude decreased the instability development time τ (the time from the start of the pulse to the instant of distortion), and at a certain $h = h_c^{(2)}$ a new distortion of somewhat different shape appeared on the trailing edge of the pulse (Fig. 3c), owing to the excitation of another parametric process. At still larger powers, oscillations appeared on the pulse, followed by a third threshold.

We interpret (see Sec. 4) the first process as the result of parametric excitation of a pair of spin waves, one of which belongs to the electronic branch and the other to the nuclear branch of the $MnCO_3$ spectrum (see Fig. 1). The second process is connected, in our opinion, with excitation of a pair of magnetoelastic oscillations. We shall henceforth call the first process the en process, and the second the ep process. We note that in a certain range of values of T and H_0 we have $h_c^{(2)} < h_c^{(1)}$ (see Fig. 8 below).

Figure 4 shows plots of the reciprocal instability development time ($1/\tau$) for both processes against the quantity $h(\tau)/h(\tau \to \infty)$ where $h(\tau \to \infty)$ is that amplitude of the field at the sample at which the development time tends to infinity (in other words, this is the threshold for the given process in the case of continuous action of the microwave signal). Both plots are straight lines, whose slope for each process separately depends little on T and H_0. The slope of the line for the en process is much larger than for the ep process. Bearing in mind the fact that the calculations pertain to the case of an infinitely long pulse, we shall present henceforth throughout the values of h_c extrapolated to $1/\tau = 0$.

Figures 5 and 6 show plots of the threshold amplitude $h_c^{(1)}$ against H_0 and T. In the field range $H_0 = 0.5$–0.75 kOe, we have $h_c^{(1)} \propto T^{1.0 \pm 0.2}$; at $H_0 = 0.5$ kOe, in particular, we have $h_c^{(1)} \propto T^{1.1 \pm 0.05}$. In the next two figures (7 and 8) we show the analogous relations for the ep process. Attention is called to the utterly different character of these relations. Figure 9 shows the dependence of the threshold amplitude ($\nu_0 = 875$ MHz) on the field for the process whose most probable cause is the excitation of nn pairs.

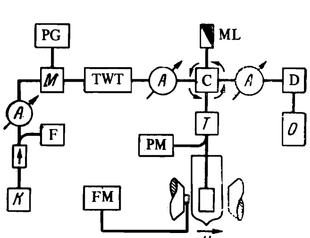

FIG. 2. Block diagram of spectrometer: A–attenuator, PG–pulse generator, D–detector, PM–power meter, FM–magnetic-field meter, K–klystron, TWT–traveling wave tube, M–microwave-power modulator, O–oscilloscope, ML–matched load, T–impedance transformer, C–circulator, F–frequency meter.

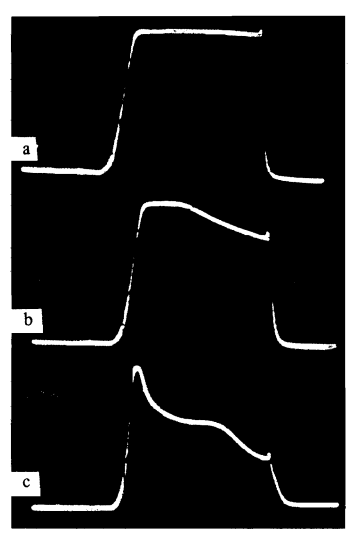

FIG. 3. Photographs of pulses reflected from the resonator at different values of the microwave magnetic field h: a) $h < h_c^{(1)}$, b) $h_c^{(1)} < h < h_c^{(2)}$, c) $h_c^{(2)} < h < h_c^{(3)}$.

Figure 10 shows the behavior of the imaginary part of the beyond-threshold susceptibility χ'' for the en and ep processes as a function of the microwave power. The absolute accuracy of the measurement of χ'' is ~50%.

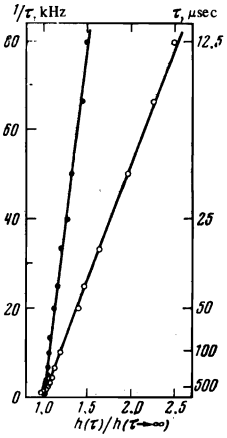

FIG. 4

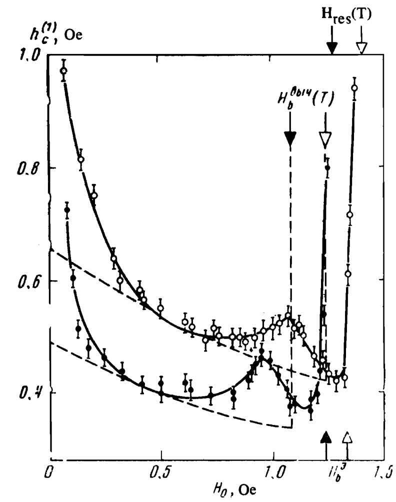

FIG. 5

FIG. 4. Dependence of the reciprocal instability-development time on the microwave magnetic field: ●—for the en process, O—for the ep process; H_0 = 500 Oe, T = 1.7°K.

FIG. 5. Plots of $h_c^{(1)}(H_0)$ at two temperatures: ●—T = 1.55°K, O—T = 2.11°K. The arrows mark the measured AFMR fields H_{res} and the limiting fields H_b calculated from formula (14) for the en process. The discrepancy between the experimental limiting fields and calculation may be due to excitation of the ep process at small $k \lesssim k_c^{(np)}$ (see Fig. 1).

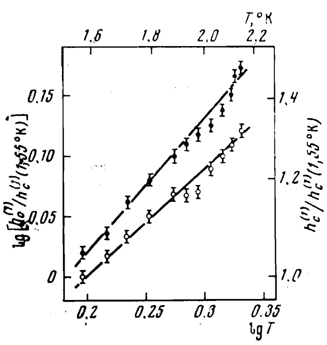

FIG. 6

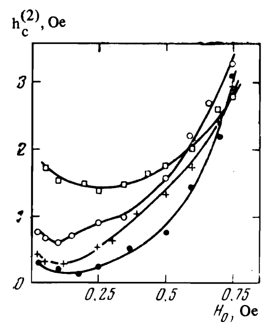

FIG. 7

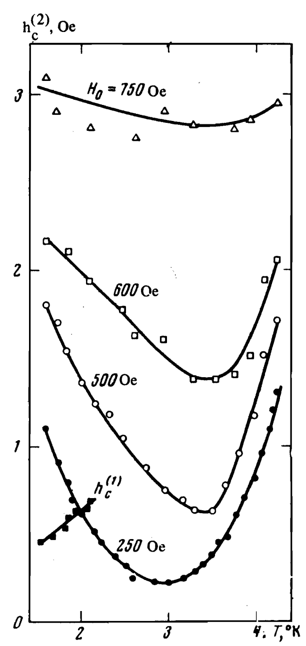

FIG. 8

FIG. 6. Temperature dependences of $h_c^{(1)}$ at ●—H_0 = 500 Oe and O—H_0 = 750 Oe. At H_0 = 0.5 we have $h_c^{(1)} \propto T^{1.1 \pm 0.05}$; at H_0 = 0.75 kOe we have $h_c^{(1)} \propto T^{0.9 \pm 0.05}$.

FIG. 7. Plots of $h_c^{(2)}(H_0)$ at different temperatures: O—1.72°K, +—2.15°K, ●—3.0°K, □—4.2°K.

FIG. 8. Temperature dependences of $h_c^{(2)}$ at various H_0; for comparison the figure shows the values of $h_c^{(1)}$ at H_0 = 250 Oe.

The region in which the instability of the beyond-threshold state is observed in the case of the ep process is shown shaded. This instability is manifest in the form of low-frequency (ν ~ 100 kHz) oscillations, and their excitation threshold h_c^{osc} is shown in Fig. 11 as a function of H_0. With decreasing H_0, the difference $h_c^{osc} - h_c^{(2)}$ increases, and the amplitude of the oscillations decreases in such a way that at $H_0 \le 0.25$ kOe they are practically unobservable. The amplitude and the fundamental frequency of the oscillations increase with increasing microwave power—see Figs. 10 and 12. We see that in

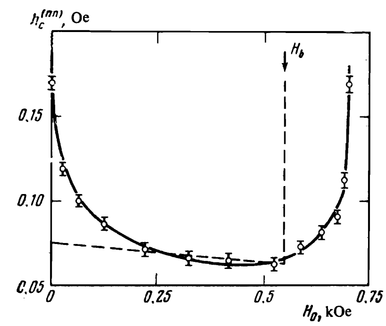

FIG. 9. Field dependence of the threshold amplitude of parallel pumping at the frequency $\omega_p = 2\pi \times 875$ MHz (T = 1.7°K). The dashed line is drawn in accordance with the formula (18c) with Q_{1nk} = const; the boundary field H_b was calculated from the condition $\omega_p = 2\Omega_{i\,nk}$. At $H_0 > H_b$, a 3–3 process with $k \lesssim k_c^{(np)}$ is possible, see Fig. 1.

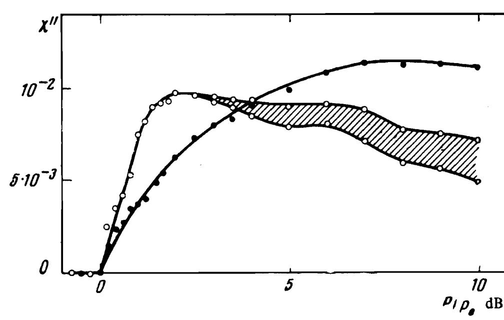

FIG. 10. Behavior of the beyond-threshold susceptibility χ'': ●—for en processes, O—for ep process; T = 1.7°K, H_0 = 500 Oe.

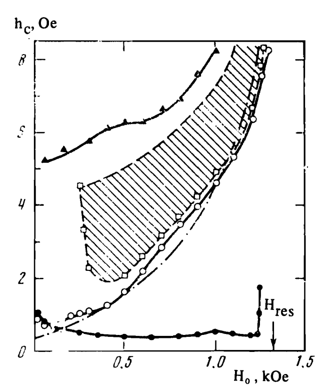

FIG. 11

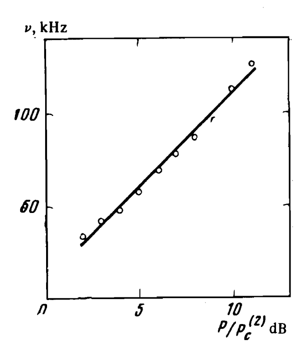

FIG. 12

FIG. 11. General picture of threshold phenomena observed in $MnCO_3$ at T = 1.7°K at the frequency $\omega_p/2\pi$ = 9.3 GHz; ●) $h_c^{(1)}$—threshold of excitation of en process; O) $h_c^{(2)}$—threshold of excitation of ep process; dash dot—result of calculations by formula (25a) for the 1–2 process; □) h_c^{osc}) oscillation excitation threshold; ▲) $h_c^{(3)}$—observed threshold of excitation of a process difficult to interpret at the present time.

FIG. 12. Dependence of the oscillation frequency of the beyond-threshold ($h > h_c^{(2)}$) susceptibility on the microwave power; H_0 = 500 Oe, T = 1.7°K.

the indicated power range we have $\nu \propto \log h$ (no spectral analysis of the oscillations was carried out). A detailed study and a discussion of the beyond-threshold phenomena are outside the scope of the present paper.

4. DISCUSSION

4A. In the case of parallel pumping in $MnCO_3$ in the $\lambda \sim 8$ mm microwave band, two peaks are observed on the $h_0(H_0)$ curve [24]. The nature of the first peak (at H_1) is still unclear, but the second (at H_2) is of phonon origin. Its position relative to the field agrees well with the calculated point $k_c^{(ep)}$ of the intersection of the softest magnons ($v_{m\perp} = 1.07 \times 10^5$ cm/sec [25]) and the softest phonons ($v_s = v_{t1} = 2.94 \times 10^5$ cm/sec [10]), see Fig. 1. The independence of H_2 of the orientation of $\mathbf{H}_0$ in the basal plane [24b] can be attributed to the almost simultaneous excitation of quasiparticles belonging to the equal-energy surface $S(\omega_p)$ in $\mathbf{k}$-space, a surface corresponding to the frequency ω_p.

The calculation undertaken in Sec. 2D pertains to excitation of single pairs. We shall plot the experimental curve $h_c^e(H_0)$ for this case by extrapolating the absorption curves $P_{out}(H_0)$ of Fig. 1a and of [17a] in the direction from H_e towards H_q to the zero-absorption level. We can attempt to describe the curve obtained in this manner, which is shown in Fig. 13, with the aid of formulas (22a) and (22b), by putting $\omega_E\omega_{med} \sim 0.4$ kOe^2 (i.e., close in order of magnitude to $\omega_E\omega_{mes} \sim 0.39$ kOe^2 as determined in [3,6]), and assuming for the Q's the values $q_{mk} \sim 10^5$ and $q_{sk} \sim 10^4$, which are reasonable at the corresponding frequencies (the boundary field H_b is calculated from (14) at $k = 0$), we can state that the agreement is qualitatively good. Allowance for the harder phonons raises the threshold at $H_2 > H_0 > H_b$. Allowance for the magnons (see (8c); $v_{m\parallel} = 1.48 \times 10^5$ m/sec [25]) raises the thresholds at $H_0 < H_2$. Allowance for four-particle interactions can explain the hardness of the excitation and the hysteresis, and can smooth out the phonon peaks (as a result of averaging of the magnon-phonon coupling over $S(\omega_p)$).

4B. Comparison of theory with experiment for the case of en and nn pumping in AFEP with the Dzyaloshinskiĭ interaction was carried out by us earlier [17b] and in Figs. 5 and 9, and demonstrates that the Dzyaloshinskiĭ interaction affects the determination of $h_c^{(en)}$ and

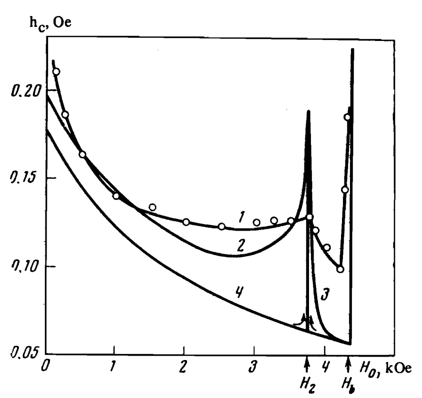

FIG. 13. For use in comparison of theory with experiment at 35 GHz. Curve 1 was plotted from the experimental data of [17a]. Curves 2 and 3 are plots of formulas (22a) and (22b) with the parameters given in the text (Sec. 4A). Curve 4 corresponds to the case when there is no magnon-phonon coupling ($\omega_{med} = 0$).

$h_c^{(nn)}$, namely, just as in the case of the ee pumping [24], the presence of this interaction makes it possible to observe parametric excitation down to very low fields H_0. Relation (19) for $MnCO_3$ does not seem to be satisfied (just as for $CsMnF_3$ [8,10]). One of the reasons may be the neglect of the linear excitation of the QAF of the n-mode. The value $(Q_{1ek}Q_{1nk})^{1/2} \sim 10^4$ obtained at $T = 1.7°$K agrees well with the data [8a] for $CsMnF_3$ (which we reduce by means of formula (18b) at $H_D = 0$). It follows therefore that the nature of the relaxation processes in $CsMnF_3$ and $MnCO_3$ is apparently the same (see also [24c]).

In view of the strong coupling between the oscillations of the E and N systems in the AFEP, it is more advantageous to characterize the relaxation by means of the values of $Q_{\nu\rho k}$ of the normal modes, and not by $q_{\nu\rho k}$ of the unperturbed oscillations, since the appreciable restructuring of the spectrum ($\omega_n - \Omega_{1nk} \sim \omega_n$) influences directly the three- and four-magnon processes, and therefore the transformation $Q_{\nu\rho k} \to q_{\nu\rho k}$ with the aid of the differentiation of (10) is too rough an approximation (for normal magnetoelastic oscillations, to the contrary, the relative restructuring of the spectrum is small even at the "intersection point," so that the use of q_{mk} and q_{sk} instead of $Q_{\sigma k}$ is not only more convenient for these oscillations, but is physically justified).

From experiment (Fig. 6) and from formulas (11) and (18b) it follows that $(Q_{1ek}Q_{1nk})^{-1} \propto T^{1.0 \pm 0.2}$ in the temperature range 1.55–2.17°K and $H_0 = 0.5$–0.75 kOe, where $k \sim 3 \times 10^5$ cm^{-1}. We note that to study the temperature dependences we have chosen values of k far from the point of intersection of the magnon and phonon branches. Calculations of the relaxation parameters from the $h_c^{(en)}(T)$ dependence as $k \to 0$ (as also in the case $h_{(ee)}(T)$, see Fig. 13 above) by formulas (18b) and (18a) can yield distorted information, owing to the neglect of the magnetoelastic coupling (including the case of the magnetostatic modes).

By studying the influence of the heating of the N system (with the aid of the NMR saturation at the frequency Ω_{1n0}, see [6]) on the value of $h_c^{(en)}$, we obtained the relation $h_c^{(en)} \propto T_n^{1.8 \pm 0.2}$, after which we found that $Q_{1ek} \propto T$, i.e., the Q of the magnons increases with increasing temperature in the interval 1.55–2.17°K. This unusual dependence can take place only if a noticeable contribution is made to the magnon relaxation by the three-particle ($e \rightleftarrows e + n$) processes with participation of nuclear spin waves (see below).

4C. Greatest interest attaches to the observation of parametric excitation with threshold $h_c^{(2)}$—see Figs. 7 and 8. This is apparently an autonomous phenomenon not connected with superheating of the system in the state that is beyond the threshold of en pumping; it is seen from Fig. 8 that, for example at $H_0 = 0.25$ kOe, the value of $h_c^{(2)}$ at $T > 2°$K becomes smaller than $h_c^{(1)}$, and that $h_c^{(2)}(T)$ does not have here a noticeable kink (although one should expect this kink from a more detailed analysis).

What is unusual is the increase of the threshold amplitude with increasing field—Fig. 7 (a similar dependence was predicted for ferrites in [19] and was observed in [27] at a frequency $\omega_p = 2\pi \times 114$ MHz), as well as the initial decrease of this amplitude with temperature—Fig. 8. These two qualitative singularities are explained under the assumption that excitation of 1–2 or 2–2 pairs of magnetoelastic oscillations takes place at $h_c^{(2)}$, see Fig. 1 (the 1—1 process is forbidden by the condition (14)), namely, a decrease of H_0 or an increase of T brings $k_{\sigma\rho}$ closer to the point $k_c^{(ep)}$, and this improves the coupling of the pairs with the pump, owing to the increase of the admixture of the E component to the deformations in the quasiphonons Ω_{2k}.

Under our experimental conditions (ω_p/γ = 3.33 kOe, T ≥ 1.55°K, H_0 ≥ 0.25 kOe), $k_{\sigma\rho}$ is situated to the left of $k_c^{(ep)}$ and is far enough to be able to put $4\omega_E\omega_{med}\omega_{sk}^2 \ll (\omega_{mk}^2 - \omega_{sk}^2)^2$ in (21). In addition, the simplification $\omega_{mk} \approx \omega_{m0}$ is possible. It follows then from (8), (14), (21), and (22) that

$$\gamma h_c^{(12)} \approx \frac{2\omega_{m0}\omega_p(2\omega_{m0}-\omega_p)}{\gamma(H_D+2H_0)(\omega_E\omega_{med})^{1/2}} \frac{1}{(q_{mk}^{(12)} q_{sk}^{(12)})^{1/2}}, \quad k_{12} \approx \frac{\omega_p-\omega_{m0}}{v}; \tag{23a}$$

$$\gamma h_c^{(22)} \approx \frac{2(\omega_{m0}^2-\omega_p^2/4)^2}{\gamma(H_D+2H_0)\omega_E\omega_{med}} \frac{1}{q_{sk}^{(22)}}, \quad k_{22} \approx \frac{\omega_p}{2v_s}. \tag{23b}$$

In the considered frequency range, the Q's of the phonons are smaller than or of the order of the Q of the magnons [28], so that we can conclude from (23) that $h_c^{(12)} < h_c^{(22)}$, i.e., the excitation of the 1—2 process precedes the 2—2 process (in contrast to the expected situation in [29]).

The plot of $h_c^{(12)}(H_0)$ for T = 1.7°K (see Fig. 11) was obtained in accordance with (28) at $\omega_E\omega_{med}q_{mk}/\gamma^2 \sim 1.6\cdot10^3$ kOe^2 and $q_{sk} \sim$ Lk, where L is the smallest dimension of the sample (~0.1 cm). The last relation is a consequence of the realistic assumption that the mean free path of the phonons at these frequencies is determined by the boundaries of the samples.

Calculation of $h_c^{(12)}(T)$ with the same values of q_{mk} and q_{sk} (which are constant with respect to T) leads at H_0 = 0.5 and 0.25 kOe to unexpectedly good description of the descending sections of the $h_c^{(2)}(T)$ curves in Fig. 8. The subsequent growth of $h_c^{(12)}$ can be easily attributed to the inevitable temperature-induced increase of q_{mk}^{-1}. From the good agreement between $h_{c\,calc}^{(12)}(T)$ and $h_{c\,obs}^{(2)}(T)$ in the region 1.55—3.4°K we can assume that in this temperature and field range there exists, besides the three- and four-particle processes of E-magnon relaxation, which make a contribution with $dq_{mk}^{-1}/dT > 0$ [30] to the total relaxation, also a process with $dq_{mk}^{-1}/dT < 0$ and of comparable intensity. One cannot exclude the possibility that this process is the three-particle (e ⇄ e + n) process mentioned in the preceding section. Its intensity decreases with increasing field and can decrease with increasing temperature, owing to the decrease of the EN coupling.

5. CONCLUSIONS

1. Antiferromagnets with easy-plane anisotropy combine the favorable properties of ferrites (relatively low natural frequencies of the electron and spin waves at ak ≪ 1) and antiferromagnets (exchange enhancement of the influences of the hyperfine and magnetoelastic interactions on the dynamics of the system).

2. Parametric excitation of pairs of normal oscillations containing not only the electron-spin but also the nuclear-spin and elastic subsystem variables, is facilitated by the exchange interaction (which as a rule is large), since the dynamic coupling (as measured by the maximum perturbation of the frequencies) is more than $(\omega_E/\omega_{1k})^{1/2}$ times larger than in ferrites.

3. The Dzyaloshinskiĭ interaction influences in equal fashion the parametric excitation of pairs of different nature in AFEP, and lowers the threshold amplitudes.

4. For magnetically ordered crystals with strong coupling of the oscillations of the electron-spin and nuclear-spin subsystems, it is of interest to study the three-wave mechanisms (with participation of nuclear spin waves) of the relaxation of electron and nuclear spin waves.

5. The most probable cause of the nonlinear process with threshold $h_c^{(2)}$ in $MnCO_3$ is excitation of nondegenerate (belonging to different branches of the spectrum) pairs of normal magnetoelastic oscillations. The conclusion requires a direct proof (for example, by extraction of the phonons from the sample), since this process can serve as a convenient means of generation of microwave (quasi) phonons with smooth frequency tuning (in a wide range) by a stationary magnetic field.

We are deeply grateful to I. K. Kikoin for constant interest in this research, to A. S. Borovik-Romanov, L. A. Prozorova, and B. Ya. Kotyuzhanskiĭ for useful discussions, and to V. D. Voronkov, G. A. Yakovlev and L. M. Yakubenya, for help in the solution of methodological problems.

APPENDIX

1. The initial expressions for the interaction energies are

$$\mathscr{H}_{EE} = 2\sum_{j_1,\delta}\{J(\delta)(\mathbf{S}_{j1}\mathbf{S}_{j2}) + \mathbf{D}(\delta)[\mathbf{S}_{j1}\mathbf{S}_{j2}] + K_2(\delta)S_{j1}^zS_{j2}^z\} + K_1\sum_{\nu,j_\nu}(S_{j\nu}^z)^2 + \hbar\gamma\mathbf{H}\sum_{\nu,j_\nu}\mathbf{S}_{j\nu}, \quad \gamma\equiv\gamma_e>0; \tag{A.1}$$

$$\mathscr{H}_{EN} = -A\sum_{\nu,j_\nu}(\mathbf{S}_{j\nu}\mathbf{I}_{j\nu}), \quad \mathscr{H}_{NN}=\mathscr{H}_{NS}=0, \quad A>0, \quad \gamma_n\approx0; \tag{A.2}$$

$$\mathscr{H}_{SS} = \mathscr{H}_{SS}^{(0)} + \mathscr{H}_{SS}^{(1)} + \hbar\sum_{s,\mathbf{k}}\omega_{s\mathbf{k}}b_{s\mathbf{k}}^+b_{s\mathbf{k}}, \quad s=1,2,3; \tag{A.3}$$

$$\mathscr{H}_{ES} = \sum_{\nu,j_\nu}\left[b_1\sum_{\lambda'}(S_{j\nu}^{\lambda'})^2u_{\lambda'\lambda'}^{(j\nu)} + b_2\sum_{\lambda'\neq\mu'}S_{j\nu}^{\lambda'}S_{j\nu}^{\mu'}u_{\lambda'\mu'}^{(j\nu)}\right], \quad u_{\lambda'\mu'}^{(j1)} = u_{\lambda'\mu'}^{(j2)} \tag{A.4}$$

Here and below, ν = 1 and 2; j_ν = 1 to N, where N is the number of sites in the sublattice; $M_0 = \gamma\hbar SNV^{-1}$ is the sublattice magnetization; M is the mass of the magnetic unit cell, $\boldsymbol{\delta} \equiv \mathbf{r}_{j_1} - \mathbf{r}_{j_2}$; $\lambda', \mu' \equiv$ x′, y′, z′ (z′ ∥ [001]); $\lambda, \mu \equiv$ x, y, z (z ∥ [111]). The Hamiltonian $\mathscr{H}_{ES}\{\lambda'\}$ is transformed into $\mathscr{H}_{ES}\{\lambda\}$ with the aid of (4.A7) of [13]:

$$u_{\lambda\mu}^{(j\nu)} = \sum_{s\mathbf{k}}\Phi_{s\mathbf{k}}^{(\lambda\mu)}(b_{s\mathbf{k}} - b_{s-\mathbf{k}}^+)\exp\{i\mathbf{k}\mathbf{r}_{j\nu}\}, \quad \Phi_{s\mathbf{k}}^{(\lambda\mu)} = \frac{i}{2}\left(\frac{\hbar}{2NM}\right)^{1/2}\omega_{s\mathbf{k}}^{-1/2}(k_\lambda\varepsilon_{s\mu} + k_\mu\varepsilon_{s\lambda}), \tag{A.5}$$

ϵ_s is a unit vector of the phonon polarization; ρV is the crystal mass (ρV = NM). The auxiliary coordinate systems (z_ν is the quantization axis) are shown in Fig. 14.

2. For the E subsystems, after going over to $a_{\nu e\mathbf{k}}^{\pm}$ and taking into account the static EN and ES interactions, we have

$$\mathscr{H}_{ee}^{(2)} = \hbar\sum_{\mathbf{k}}\{A_{\mathbf{k}}(a_{1e\mathbf{k}}^{\pm}a_{1e\mathbf{k}} + a_{2e\mathbf{k}}^{\pm}a_{2e\mathbf{k}}) + B_{\mathbf{k}}(a_{1e\mathbf{k}}a_{2e-\mathbf{k}} + a_{1e\mathbf{k}}^{\pm}a_{2e\mathbf{k}}^{\pm})$$

$$+C_{\mathbf{k}}(a^+_{1e\mathbf{k}}a_{2e\mathbf{k}}+a_{1e\mathbf{k}}a^+_{2e\mathbf{k}})+{}^1/{}_2D_{\mathbf{k}}(a_{1e\mathbf{k}}a_{1e-\mathbf{k}}+a_{2e\mathbf{k}}a_{2e-\mathbf{k}}+\mathrm{H.c.})\};$$

$$A_{\mathbf{k}}\equiv\gamma(H_E\cos 2\psi+H_D\sin 2\psi+H_{A1}+H_N+H_{mes}+H_0\sin\psi), \qquad (\mathrm{A.6})$$

$$B_{\mathbf{k}}\equiv\frac{S}{2\hbar}\sum_{\delta}f^+(\delta)e^{i\mathbf{k}\delta},\quad C_{\mathbf{k}}\equiv\frac{S}{2\hbar}\sum_{\delta}f^-(\delta)e^{i\mathbf{k}\delta},\quad D_k\equiv\gamma H_{A1},$$

where

$$f^\pm(\delta)=2[J(\delta)\cos 2\psi+D(\delta)\sin 2\psi]\pm 2[J(\delta)+K_2(\delta)],$$

$H_{A1}\equiv K_1S/\hbar\gamma$, $H_{mes}\equiv\omega_{mes}/\gamma$ is the effective field of the static magnetoelastic coupling (see[4]); $H_N = A\langle I^{z\nu}\rangle/\hbar\gamma\equiv\omega_N/\gamma$, $\omega_n = AS/\hbar$ is the frequency of the "unshifted" NMR, $\omega_{en}\equiv(\omega_n\omega_N)^{1/2}$, $\langle I^{z\nu}\rangle = \hbar\omega_n I(I+1)/3k_BT$.

Taking into account interactions only between the nearest neighbors (their number is $\zeta = 6$ for $MnCO_3$) and putting $J(\delta_1) = J$, $D(\delta_1) = D$, $K_2(\delta_1) = K_2$, we introduce

$$H_E=\frac{2\zeta JS}{\hbar\gamma}=\frac{\omega_E}{2\gamma},\quad H_D\equiv\frac{2D\zeta S}{\hbar\gamma},\quad H_{A2}=\frac{2K_2S\zeta}{\hbar\gamma},$$
$$H_A=2H_{A1}-H_{A2}. \qquad (\mathrm{A.7})$$

The balance equations take the form

$$H_E\sin 2\psi-H_D\cos 2\psi=H_0\cos\psi. \qquad (\mathrm{A.8})$$

The frequencies of the "pure" waves in the E system are equal to

$$\omega_{\nu\mathbf{k}}^2=[A_{\mathbf{k}}+(-1)^\nu C_{\mathbf{k}}]^2-[B_{\mathbf{k}}+(-1)^\nu D_{\mathbf{k}}]^2. \qquad (\mathrm{A.9})$$

The conversion coefficients (5a) are as follows

$$\mathrm{S}=\begin{pmatrix}\mathrm{S}_u & \mathrm{S}_v\\ \mathrm{S}_v^* & \mathrm{S}_u^*\end{pmatrix},\quad \mathrm{S}_u=\begin{pmatrix}U_{1\mathbf{k}} & U_{2\mathbf{k}}\\ -U_{1\mathbf{k}} & U_{2\mathbf{k}}\end{pmatrix},\quad \mathrm{S}_v=\begin{pmatrix}V_{1\mathbf{k}} & -V_{2\mathbf{k}}\\ -V_{1\mathbf{k}} & -V_{2\mathbf{k}}\end{pmatrix} \qquad (\mathrm{A.10})$$

where

$$U_{\nu\mathbf{k}}=\left[\frac{A_{\mathbf{k}}+(-1)^\nu C_{\mathbf{k}}+\omega_{\nu\mathbf{k}}}{4\omega_{\nu\mathbf{k}}}\right]^{1/2},\quad V_{\nu\mathbf{k}}=\left[\frac{A_{\mathbf{k}}+(-1)^\nu C_{\mathbf{k}}-\omega_{\nu\mathbf{k}}}{4\omega_{\nu\mathbf{k}}}\right]^{1/2}$$
$$U_{\nu\mathbf{k}}^2-V_{\nu\mathbf{k}}^2=1/2.$$

3. The coefficients of the Hamiltonian (7) are

$$E_{\nu\mathbf{k}}=2(U_{\nu\mathbf{k}}^2+V_{\nu\mathbf{k}}^2)\omega_n,\quad G_{\nu\mathbf{k}}=-2(U_{\nu\mathbf{k}}^2+V_{\nu\mathbf{k}}^2)\omega_{en},$$
$$F_{\nu\mathbf{k}}=-(-1)^\nu\cdot 4U_{\nu\mathbf{k}}V_{\nu\mathbf{k}}\omega_n,\quad H_{\nu\mathbf{k}}=(-1)^\nu\cdot 4U_{\nu\mathbf{k}}V_{\nu\mathbf{k}}\omega_{en}. \qquad (\mathrm{A.11})$$

At small cant angles ($\psi\ll 1$) we have

$$D_{1s\mathbf{k}}\approx -i\frac{(U_{1\mathbf{k}}+V_{1\mathbf{k}})S^{3/2}}{(M\hbar\omega_{s\mathbf{k}})^{1/2}}\left[\frac{b_1+2b_2}{3}(k_x\varepsilon_{sy}+k_y\varepsilon_{sx})-\frac{\sqrt{2}}{3}(b_1-b_2)(k_y\varepsilon_{sz}+k_z\varepsilon_{sy})\right]$$

$$D_{2s\mathbf{k}}\approx -\frac{(U_{2\mathbf{k}}+V_{2\mathbf{k}})S^{3/2}}{(M\hbar\omega_{s\mathbf{k}})^{1/2}}\left[\frac{2b_1+b_2}{3}(k_y\varepsilon_{sz}+k_z\varepsilon_{sy})-\frac{\sqrt{2}}{3}(b_1-b_2)(k_x\varepsilon_{sy}+k_y\varepsilon_{sx})\right].$$

The connection with the notation of[13] is the following: $M = \rho VN^{-1}$, $2NS^2b_{1,2} = VB_{1,2}$.

The Hamiltonians of the perturbation in (2) take the form

$$\mathcal{H}_3\approx\mathcal{H}_{eee}^{(3)}\approx\frac{\gamma\hbar H_0\cos\psi}{(2NS)^{1/2}}\sum_{\mathbf{k}_1,\mathbf{k}_2,\mathbf{k}_3}\gamma_{\mathbf{k}_1}[(a_{1e\mathbf{k}_1}+a^+_{1e-\mathbf{k}_1})a^+_{2e-\mathbf{k}_2}a_{2e\mathbf{k}_3}$$
$$+(a_{2e\mathbf{k}_1}+a^+_{2e-\mathbf{k}_1})a^+_{1e-\mathbf{k}_2}a_{1e\mathbf{k}_3}]\Delta(\mathbf{k}_1+\mathbf{k}_2+\mathbf{k}_3), \qquad (\mathrm{A.12})$$
$$\gamma_{\mathbf{k}}\equiv\frac{1}{\zeta}\sum_{\langle nn\rangle}e^{i\mathbf{k}\delta};$$

$$\mathcal{H}'\approx\mathcal{H}_e'\approx\gamma\hbar h\cos(\omega_pt)\left(\frac{SN}{2}\right)^{1/2}\cos\psi\cdot(a_{1e0}+a^+_{1e0}+a_{2e0}+a^+_{2e0})$$
$$+\gamma\hbar h\cos(\omega_pt)\sin\psi\sum_{\mathbf{k}}(a^+_{1e\mathbf{k}}a_{1e\mathbf{k}}+a^+_{2e\mathbf{k}}a_{2e\mathbf{k}}). \qquad (\mathrm{A.13})$$

4. Diagonalization of the hyperfine interaction yields

$$X_\nu=R_\nu X_\nu',$$
$$X_\nu\equiv(c_{\nu e\mathbf{k}},c_{\nu n\mathbf{k}},c^+_{\nu e-\mathbf{k}},c^+_{\nu n-\mathbf{k}})^T, \qquad (\mathrm{A.14})$$
$$X_\nu'\equiv(\alpha_{\nu e\mathbf{k}},\alpha_{\nu n\mathbf{k}},\alpha^+_{\nu e-\mathbf{k}},\alpha^+_{\nu n-\mathbf{k}})^T$$

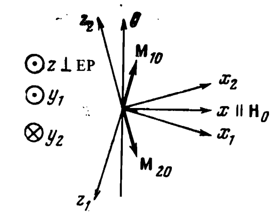

FIG. 14. Principal and auxiliary coordinate systems.

(ν = 1 or 2, i.e., we are considering here also the QAF mode). Using in the calculations the symmetry properties of the matrix R, which are indicated in[12], we obtain

$$\mathrm{R}_\nu=\begin{pmatrix}\mathrm{R}_\nu' & \mathrm{R}_\nu''\\ \mathrm{R}_\nu''^* & \mathrm{R}_\nu'^*\end{pmatrix},\quad \mathrm{R}_\nu'=\begin{pmatrix}1 & f_{\nu\mathbf{k}}'\\ -g_{\nu\mathbf{k}}' & W_{\nu\mathbf{k}}\end{pmatrix},$$
$$\mathrm{R}_\nu''=(-1)^\nu\begin{pmatrix}\sigma_{\nu\mathbf{k}} & f_{\nu\mathbf{k}}''\\ -g_{\nu\mathbf{k}}'' & (W_{\mathbf{k}}^2-1)^{1/2}\end{pmatrix}.$$

At $(\omega_{\nu\mathbf{k}}^2/\omega_E\omega_N-1)\gg\omega_n/\omega_E$, putting $\rho_{\nu\mathbf{k}}\equiv\omega_{en}/\omega_{\nu\mathbf{k}}$, we obtain: in case I (strong coupling, $\omega_E/4\omega_{\nu\mathbf{k}}\gg 1$—see Sec. 2C)

$$W_{\nu\mathbf{k}}=\left(\frac{\Omega_{\nu n\mathbf{k}}\omega_E}{4\omega_n\omega_{\nu\mathbf{k}}}\right)^{1/2},\quad \sigma_{\nu\mathbf{k}}=\frac{\rho_{\nu\mathbf{k}}^2\omega_n\omega_E}{4\omega_{\nu\mathbf{k}}^2}\ll 1,$$
$$f_{\nu\mathbf{k}}\equiv f_{\nu\mathbf{k}}'=f_{\nu\mathbf{k}}''=\rho_{\nu\mathbf{k}}\left(\frac{\omega_n\omega_E}{4\Omega_{\nu n\mathbf{k}}\omega_{\nu\mathbf{k}}}\right)^{1/2}, \qquad (\mathrm{A.14A})$$
$$g_{\nu\mathbf{k}}'=g_{\nu\mathbf{k}}''=\frac{\rho_{\nu\mathbf{k}}\omega_E}{2\omega_{\nu\mathbf{k}}};$$

and in the case II (weak coupling, $\omega_E/4\omega_{\nu\mathbf{k}}\gtrsim 1$) with relative accuracy $\rho\nu^2$ we have

$$W_{\nu\mathbf{k}}=U_{\nu\mathbf{k}}\sqrt{2},\quad f_\nu'=\rho_{\nu\mathbf{k}}U_{\nu\mathbf{k}}\sqrt{2},\quad f_{\nu\mathbf{k}}''=\rho_{\nu\mathbf{k}}V_{\nu\mathbf{k}}\sqrt{2},$$
$$g_{\nu\mathbf{k}}'=\rho_{\nu\mathbf{k}}\cdot 2(U_{\nu\mathbf{k}}^2+V_{\nu\mathbf{k}}^2),\quad g_{\nu\mathbf{k}}''=\rho_{\nu\mathbf{k}}\cdot 4U_{\nu\mathbf{k}}V_{\nu\mathbf{k}}. \qquad (\mathrm{A.14B})$$

The coupling coefficients of the normal en modes with pumping and QAF mode are expressed in terms of $U_{\nu\mathbf{k}_1}V_{\nu\mathbf{k}}$, and at $\omega_E\gg 4\omega_{\nu\mathbf{k}}$ their values are

$$F_{\mathbf{k}}^{(ee)}=\frac{\gamma(H_0+H_D)}{4\omega_{1\mathbf{k}}},\quad F_{\mathbf{k}}^{(en)}=F_{\mathbf{k}}^{(ne)}\approx 2f_{1\mathbf{k}}F_{\mathbf{k}}^{(ee)},\quad F_{\mathbf{k}}^{(nn)}\approx 4f_{1\mathbf{k}}^2F_{\mathbf{k}}^{(ee)},$$
$$R_0\Phi_{\mathbf{k}}^{(ee)}\approx\frac{\gamma H_0(\omega_{20}-2\omega_{1\mathbf{k}})}{8\omega_{1\mathbf{k}}},\quad R_0\Psi_{\mathbf{k}}^{(ee)}\approx\frac{\gamma H_0(\omega_{20}+2\omega_{1\mathbf{k}})}{8\omega_{1\mathbf{k}}}$$
$$R_0\Phi_{\mathbf{k}}^{(en)}=R_0\Phi_{\mathbf{k}}^{(ne)}\approx\frac{2f_{1\mathbf{k}}\gamma H_0(\omega_{20}-\omega_{1\mathbf{k}})}{8\omega_{1\mathbf{k}}}, \qquad (\mathrm{A.15})$$
$$R_0\Psi_{\mathbf{k}}^{(en)}=R_0\Psi_{\mathbf{k}}^{(ne)}\approx\frac{2f_{1\mathbf{k}}\gamma H_0(\omega_{20}+\omega_{1\mathbf{k}})}{8\omega_{1\mathbf{k}}},$$
$$R_0\Phi_{\mathbf{k}}^{(nn)}=R_0\Psi_{\mathbf{k}}^{(nn)}\approx\frac{4f_{1\mathbf{k}}^2\gamma H_0\omega_{20}}{8\omega_{1\mathbf{k}}}.$$

5. Diagonalization of the magnetoelastic interaction for the QF mode yields

$$\mathrm{Y}=\mathrm{TY}'$$
$$\mathrm{Y}\equiv(c_{1\mathbf{k}},b_{s\mathbf{k}},c^+_{1-\mathbf{k}},b^+_{s-\mathbf{k}})^T,\quad \mathrm{Y}'\equiv(\alpha_{1\mathbf{k}},\alpha_{2\mathbf{k}},\alpha^+_{1-\mathbf{k}},\alpha^+_{2-\mathbf{k}})^T; \qquad (\mathrm{A.16})$$
$$\mathrm{T}=\begin{pmatrix}\mathrm{T}_+ & \mathrm{T}_-\\ \mathrm{T}_-^* & \mathrm{T}_+^*\end{pmatrix}.$$

At $\psi\ll 1$, where $D^*_{1s\mathbf{k}}\approx -D_{1s\mathbf{k}}$, we have

$$\mathrm{T}_+=\begin{pmatrix}u_+ & p_+\\ iv_+ & -iq_+\end{pmatrix},\quad \mathrm{T}_-=\begin{pmatrix}-u_- & p_-\\ -iv_- & -iq_-\end{pmatrix}.$$

Putting $\Delta\equiv(\Omega_{1\mathbf{k}}^2-\Omega_{2\mathbf{k}}^2)^{1/2}$, we obtain

$$u_\pm=\frac{\Omega_{1\mathbf{k}}\pm\omega_{1\mathbf{k}}}{2\Delta}\left(\frac{\Omega_{1\mathbf{k}}^2-\omega_{s\mathbf{k}}^2}{\Omega_{1\mathbf{k}}\omega_{1\mathbf{k}}}\right)^{1/2},$$
$$p_\pm=\frac{\omega_{1\mathbf{k}}\pm\Omega_{2\mathbf{k}}}{2\Delta}\left(\frac{\omega_{s\mathbf{k}}^2-\Omega_{2\mathbf{k}}^2}{\Omega_{2\mathbf{k}}\omega_{1\mathbf{k}}}\right)^{1/2},$$
$$v_\pm=\frac{\Omega_{1\mathbf{k}}\pm\omega_{s\mathbf{k}}}{2\Delta}\left(\frac{\Omega_{1\mathbf{k}}^2-\omega_{1\mathbf{k}}^2}{\Omega_{1\mathbf{k}}\omega_{s\mathbf{k}}}\right)^{1/2}$$

$$q_\pm=\frac{\omega_{sk}\pm\Omega_{2k}}{2\Delta}\left(\frac{\omega_{1k}^2-\Omega_{2k}^2}{\Omega_{2k}\omega_{sk}}\right)^{1/2}.$$

All these numbers are positive (see Fig. 1).

Useful consequences of Eq. (21) are:

$$(\Omega_{1k}^2-\omega_{1k}^2)(\omega_{1k}^2-\Omega_{2k}^2)=(\Omega_{1k}^2-\omega_{sk}^2)(\omega_{sk}^2-\Omega_{2k}^2)=\omega_E\omega_{med}\omega_{sk}^2.$$

The coefficients of the coupling of the normal magnetoelastic modes with the pump and with the QAF mode at $\psi \ll 1$, $ak \ll 1$, $\omega_{20} \ll \omega_E$ (not only in the case $\omega_p \ll \omega_{20}$ when $\omega_{1k} \ll \omega_{20}$) take the form

$$\begin{gathered}
F_k^{(\sigma\sigma)}=\frac{\gamma(H_0+H_D)}{4\Omega_{\sigma k}}\frac{\Omega_{\sigma k}^2-\omega_{sk}^2}{\Omega_{\sigma k}^2-\Omega_{\rho k}^2}\quad(\sigma\neq\rho),\\
F_k^{(12)}=F_k^{(21)}=\frac{\gamma(H_0+H_D)\,\omega_{sk}(\omega_E\omega_{med})^{1/2}}{4(\Omega_{1k}^2-\Omega_{2k}^2)(\Omega_{1k}\Omega_{2k})^{1/2}},\\
\Phi_k^{(\sigma\rho)}=\Phi_k^{(\rho\sigma)}=\Psi_k^{(\sigma\rho)}=\Psi_k^{(\rho\sigma)}=\frac{H_0}{H_0+H_D}\frac{\omega_{20}}{2R_0}F_k^{(\sigma\rho)},\\
R_0\equiv(NS\omega_{20}/\omega_E)^{1/2},\quad \sigma,\ \rho=1,\ 2.
\end{gathered}\tag{A.17}$$

---

1) In $CsMnF_3$ in fields $H_\parallel > H_{SF}$ (~0.1 kOe), the magnetic sublattices are in the "spin-flop" state, which in many respects is similar to the equilibrium configuration in the AFEP. The same pertains to the cubic $RbMnF_3$ [10].

2) Formulas (2) and (5) of [17b] were garbled by the typesetter—they should be of the same form as (8a) and (18b).

3) It can be improved also by means of the "rhombohedral" form $\mathcal{H}_{EE}$, without assuming elastic isotropy ($c_{11}-c_{12} \neq 2c_{44}$).

1 A. S. Borovik-Romanov and L. A. Prozorova, J. de Phys., Suppl. 32, fasc. 2–3, C1–829, 1971.
2 V. I. Ozhogin, a) Zh. Eksp. Teor. Fiz. 48, 1307 (1965) [Sov. Phys.-JETP 21, 874 (1965)]; b) ibid. 58, 2079 (1970) [31, 1121 (1970)].
3 A. S. Borovik-Romanov, N. M. Kreines, and L. A. Prozorova, Zh. Eksp. Teor. Fiz. 45, 64 (1963) [Sov. Phys.-JETP 18, 46 (1964)].
4 A. S. Borovik-Romanov and E. G. Rudashevskiĭ, Zh. Eksp. Teor. Fiz. 47, 2095 (1965) [Sov. Phys.-JETP 20, 1407 (1966)].
5 E. A. Turov and M. P. Petrov, YaMR v ferritakh i antiferromagnetikakh (NMR in Ferrites and Antiferromagnets), Nauka (1969).
6 V. A. Tulin, Zh. Eksp. Teor. Fiz. 55, 831 (1968) [Sov. Phys.-JETP 28, 431 (1969)].
7 V. I. Ozhogin and P. P. Maximenkov, IEEE Trans. on Magn., MAG-8, 645, 1972.
8 M. H. Seavey, a) J. Appl. Phys. 40, 1597, 1969; b) Phys. Rev. Lett. 23, 132, 1969; c) Solid State Comm. 10, 219, 1972.
9 V. R. Gakel', ZhETF Pis. Red. 17, 75 (1973) [JETP Lett. 17, 51 (1973)].
10 L. W. Hinderks and P. M. Richards, a) J. Appl. Phys. 39, 824, 1968; b) Phys. Rev. 183, 575, 1969; c) J. Appl. Phys. 42, 1516, 1971; d) B. T. Adams, L. W. Hinderks, and P. M. Richards, J. Appl. Phys. 41, 931, 1970.
11 L. A. Prozorova and A. S. Borovik-Romanov, ZhETF Pis. Red. 10, 316 (1969) [JETP Lett. 10, 201 (1969)].
12 R. M. White, M. Sparks, and I. Ortenburger, Phys. Rev. 139, A450, 1965.
13 R. Le Crow and R. Comstock, in: Physical Acoustics, W. Mason, ed. (Russ. transl.), Mir, 1968 [Academic Press].
14 P. Fedders, Phys. Rev. B1, 3756, 1970.
15 K. Mizushima and A. Iida, J. Phys. Soc. Japan 21, 1521, 1966.
16 A. Platzker and F. R. Morgenthaler, J. Appl. Phys. 41, 927, 1970.
17 V. I. Ozhogin and A. Yu. Yakubovskiĭ, a) Zh. Eksp. Teor. Fiz. 63, 2155 (1972) [Sov. Phys.-JETP 36, 1138 (1973)]; b) Phys. Lett. 43A, 505 (1973); c) Mezhdunar. konf. po magnetizmu (Internat. Conf. on Magnetism), Moscow (1973), 23a-Y3.
18 V. G. Bar'yakhtar, M. A. Savchenko, V. V. Gann, and P. V. Ryabko, Zh. Eksp. Teor. Fiz. 47, 1989 (1964) [Sov. Phys.-JETP 20, 1335 (1965)].
19 R. L. Comstock, J. Appl. Phys. 35, 2427, 1964.
20 V. V. Kveder, B. Ya. Kotyuzhanskiĭ, and L. A. Prozorova, Zh. Eksp. Teor. Fiz. 63, 2205 (1972) [Sov. Phys.-JETP 36, 1165 (1973)].
21 R. I. Joseph, C. P. Hartwig, T. Kohane, and E. Schlömann, J. Appl. Phys. 37, 1069, 1966.
22 H. Le Gall, B. Lemaire, and D. Sere, Solid State Comm. 5, 919, 1967.
23 V. E. Zakharov, V. S. L'vov, and S. S. Starobinets, Zh. Eksp. Teor. Fiz. 59, 1200 (1970) [Sov. Phys.-JETP 32, 656 (1971)].
24 B. Ya. Kotyuzhanskiĭ and L. A. Prozorova, a) ZhETF Pis. Red. 13, 430 (1971) [JETP Lett. 13, 305 (1971)]; b) Zh. Eksp. Teor. Fiz. 62, 2199 (1972) [Sov. Phys.-JETP 35, 1050 (1972)]; c) Zh. Eksp. Teor. Fiz. 65, 2470 (1973) [Sov. Phys.-JETP 38, 1233 (1974)].
25 T. M. Holden, E. C. Svensson, and P. Martel, Canad. J. Phys. 50, 687, 1972.
26 F. A. Olson, J. Appl. Phys. 34, 1281, 1963.
27 J. P. Sage, J. Appl. Phys. 42, 343, 1971.
28 W. Strauss, J. Appl. Phys. 36, 1243, 1965.
29 R. L. Comstock and E. Hansen, J. Appl. Phys. 36, 1567, 1965.
30 V. G. Bar'yakhtar and V. L. Sobolev, Fiz. Tverd. Tela 15, 2651 (1973) [Sov. Phys.-Solid State 15, 1764 (1974)].

Translated by J. G. Adashko
37